

Harmonic and anharmonic oscillations investigated by using a microcomputer-based Atwood's machine

Barbara Pecori

Phys. Department of Bologna University, Italy

Giacomo Torzo^{a)} and Andrea Sconza

Phys. Department of Padova University, Italy

(Received 11 February 1998; accepted 26 August 1998)

We describe how the Atwood's machine, interfaced to a personal computer through a rotary encoder, is suited for investigating harmonic and anharmonic oscillations, exploiting the buoyancy force acting on a body immersed in water. We report experimental studies of oscillators produced by driving forces of the type $F = -kx^n$ with $n = 1, 2, 3$, and $F = -k \operatorname{sgn}(x)$. Finally we suggest how this apparatus can be used for showing to the students a macroscopic model of interatomic forces.

© 1999 American Association of Physics Teachers.

I. INTRODUCTION

Simple Harmonic Motion (SHM) is usually studied in introductory physics courses because it involves easy mathematics and because two simple experiments may be used as examples: the pendulum and the spring-mass system. Experimental studies are often based only on measurements of the period from which the dynamic parameters of the system are derived.

However, in real systems the linear behavior, implicit in SHM, is rarely obeyed: most oscillators are only approximately harmonic (in the small-amplitude limit) while some interesting features may only be explained if anharmonicity is taken into account (e.g., the expansion coefficient and the specific heat of solids, jumping phenomena, transition to chaos,...).

To investigate anharmonic oscillations we may study the pendulum where the restoring force is $F = -mg \sin \Phi$: by retaining the first two terms of the series expansion $\sin \Phi = \Phi - \Phi^3/6 + \dots$; we get¹ $F = \approx -mg(\Phi - \Phi^3/6) = -\kappa\Phi + \kappa'\Phi^3$.

A particular feature of the pendulum is that the restoring force mimics that of a spring that *softens* at larger amplitudes. Real springs, on the contrary, become *stiffer* at larger amplitudes, the restoring force being $F = -kx - k'x^3$. Both in the pendulum and in the mass-spring system the ratio between the cubic and the linear term cannot be freely varied: it is constant ($\kappa'/\kappa = -\frac{1}{6}$) in one case, while it depends on the mechanical properties of the spring material in the other.²

A simple way to explore both harmonic and anharmonic oscillations, with a free and easy choice of the system anharmonicity, is to use a modified Atwood's machine, where one of the two masses hanging from the pulley drops into a water bath.

The essential feature of this setup is that, since Archimedes' force is a function of the immersed body volume, the behavior of the restoring force $F(x)$ can be changed by modifying the body shape.

In this paper we report some experiments involving various types of restoring forces, all of them exploiting the buoyancy effect.

The physical model of this modified Atwood's machine is described in Sec. II; we derive from the model the main

features of the motion of an oscillating cylinder for small amplitudes ($F = -kx$) in Sec. II A and for large amplitudes ($F = -k \operatorname{sgn} x$) in Sec. II B; in Sec. II C we study the case of an oscillating triangle ($F = -kx - k'x^2$) and in Sec. II D the case of an oscillating cone ($F = -kx + k'x^2 - k''x^3$). In Sec. III we describe the experimental setup and in Sec. IV the procedure used to characterize the system. In Sec. V we report the data obtained for the different types of oscillations, we compare the predictions provided by the models with the experimental results, and we exploit the discrepancies to refine the models. Conclusions are drawn in Sec. VI and a calculation of the period versus amplitude for various restoring forces is reported in the Appendix.

II. OSCILLATIONS WITH THE ATWOOD'S MACHINE

The Atwood's machine is a device where two masses hang from the ends of a string passing over a pulley that can freely rotate on its horizontal axis.

In the apparatus used in this study one of the two masses (m_2 with volume V_2) dips into a water bath (Fig. 1).

The motion of the whole system can be simply described by the motion of the mass m_2 : here we use an orthogonal reference frame with a downward directed vertical axis.

If we assume a massless and inextensible string, the linear acceleration a of the mass m_2 may be calculated by equating the torque \mathcal{T} applied to the pulley to the rate of change of its angular momentum $d(I\omega)/dt$:

$$\mathcal{T} = R(\tau_2 - \tau_1) = d(I\omega)/dt, \quad (1)$$

where $\mathcal{T} = R(\tau_2 - \tau_1)$ is the net driving torque in the absence of friction, R is the pulley's radius, I is the momentum of inertia, and τ_1 and τ_2 are the tensions applied to the string by the masses m_1 and m_2 , respectively.

The pulley's angular momentum is $L = I\omega$, where $v = \omega R$ relates the linear velocity v of m_2 to the pulley's angular velocity ω (in the absence of wire slipping).

Each one of the string's tensions is related to the acceleration a and to the other forces applied to each body, by the Newton's law:

$$\tau_1 = m_1(a + g) \quad \text{and} \quad \tau_2 = m_2(g - a) - F_A(h), \quad (2)$$

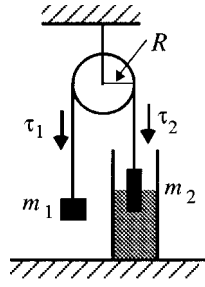


Fig. 1. Schematic of the Atwood's machine.

where $F_A(h)$ is the Archimedes force that, being proportional to the volume of the displaced water, is a function of the immersed height h .

Relations (2) may be used to eliminate τ_1 and τ_2 from Eq. (1),

$$R(\tau_2 - \tau_1) = R[(m_2 - m_1)g - (m_2 + m_1)a - F_A(h)]/dt = Ia/R, \quad (3)$$

giving

$$a = \frac{\Delta m g - F_A(h)}{m_1 + m_2 + I/R^2}. \quad (4)$$

If $\Delta m = m_2 - m_1$ is less than ρV_2 (where ρ is the water density), the Archimedes force balances the gravity force $\Delta m g$ for some value h_0 of the immersed height h : $F_A(h_0) = \Delta m g$, and for any displacement from the equilibrium position the restoring force F acting on the system is the opposite of the change of the buoyancy force $\Delta F_A = F_A(h) - \Delta m g$. In fact, when the body dips (positive displacement) the buoyancy force increases (i.e., its change is positive) and the restoring force is directed upward (i.e., is negative in the chosen reference frame): $F = -\Delta F_A$.

If we define $\mathcal{M} = m_1 + m_2 + I/R^2$ as the total inertial mass of the system,³ the acceleration may be written as

$$a = -\Delta F_A / \mathcal{M}. \quad (5)$$

If we want to take into account the effect of dissipative forces, we may add to the driving torque $T = R(\tau_2 - \tau_1)$ a friction torque $T_f = \pm R F_F$, where with F_F we define an effective friction force (directed opposite to v_2) applied to m_2 . In this case the acceleration a' of m_2 may be written as

$$a' = a \pm F_F / \mathcal{M}, \quad (6)$$

where the \pm sign depends on the direction of the velocity, which may be the same as or opposite to that of the acceleration.

A. Harmonic oscillations of a cylinder: $F = -kX$

When the body m_2 is a cylinder of radius r , the Archimedes force is $F_A(h) = \pi r^2 h \rho g$, and its change ΔF_A may be written as a function of the displacement $X = h - h_0$ from the equilibrium position: $\Delta F_A(X) = \pi r^2 \rho g (h_0 + X) - \pi r^2 h_0 \rho g = \pi r^2 \rho g X$.

This system is equivalent to the well-known mass-spring system, the "elastic constant" being determined by the cylinder radius r and by the liquid density ρ .

From relation (5) we obtain the cylinder acceleration:

$$a = -(k/\mathcal{M})X, \quad (7)$$

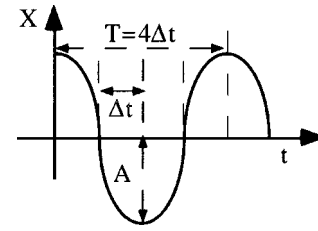


Fig. 2. The displacement versus time plot for an oscillator $F = -k \operatorname{sgn}(x)$.

where $k = \pi r^2 \rho g$, showing that we are dealing with a simple harmonic motion whose period is

$$T = 2\pi \sqrt{\mathcal{M}/k} = 2\pi \sqrt{\mathcal{M}/\pi r^2 \rho g}. \quad (8)$$

In other words, as the cylinder rises above its equilibrium point, the Archimedes force decreases because a smaller volume is displaced. This increases the downward force, and causes the cylinder to fall. If it drops below its equilibrium point, the Archimedes force increases because a greater volume is displaced; this causes the upward force to increase and the cylinder to rise.

This description of the motion is valid as long as the oscillation amplitude does not exceed an upper limit above which the cylinder is completely immersed or completely out of the water.

B. Oscillations due to a constant restoring force: $F = -k \operatorname{sgn} X$

If the oscillation amplitude is made very large ($X \gg l$, where l is the cylinder length): the cylinder spends most of the time completely outside or completely inside the water bath, and in each case the restoring force is constant. In fact, the restoring force when the whole cylinder is outside water is $\Delta m g$ and when the whole cylinder is inside water is $\Delta m g - F_A(l) = \Delta m g [(h_0 - l)/h_0]$.

If we want to obtain a motion that is symmetric around the equilibrium point, we must let $h_0 = l/2$. In this case, if we neglect the short transient during which the cylinder is partially immersed, the absolute value of the force $\pi(l/2)r^2 \rho g = \Delta m g$ remains constant while its sign changes when the cylinder crosses the water surface:

$$F = -k \operatorname{sgn}(X), \quad (9)$$

where $k = \pi(l/2)r^2 \rho g$ and the acceleration is

$$a = \pm k/\mathcal{M} = \pm \pi(l/2)r^2 \rho g/\mathcal{M}. \quad (10)$$

In this type of oscillation⁴ the period is directly proportional to the square root of the amplitude A , as may be easily seen by inspecting Fig. 2. The $X(t)$ graph is made, in fact, of parabolic branches ($X = at^2/2$), and within each branch the relation between the base Δt and the height A is described by the equation $A = a \Delta t^2/2$. The period is therefore

$$T = 4 \Delta t = 4 \sqrt{2A/a} = 8 \sqrt{\mathcal{M}/(\pi r^2 l \rho g)} \sqrt{A}. \quad (11)$$

C. Oscillations of twin triangles: $F = -k|X|X$

If we use, instead of a body with constant cross section, a body whose cross section changes linearly, the buoyancy forces increases quadratically with depth.

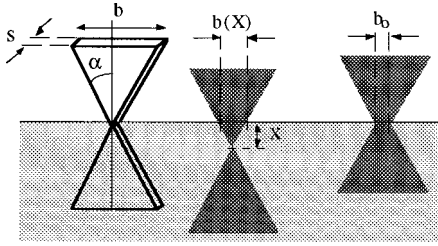


Fig. 3. Schematics of the body shaped as twin triangles.

Suppose our body is a slab in the shape of twin triangles attached at their vertex and that the counterweight is chosen to keep the twin triangles in equilibrium *half-submerged* in the water bath.

When the twin triangles are displaced by a length X from equilibrium, the change in the displaced water volume may be written by $\Delta V(X) = sb(X)X/2 = sB|X|(\tan \alpha)X$, where B is the triangle base, s the thickness, α the aperture angle, and $sb(X) = 2s(\tan \alpha)|X|$ the cross section at the distance X from the vertex (Fig. 3).

We are here assuming $b(0) = 0$, i.e., a zero cross section at the twin triangles' vertex, so that the restoring force $F = -\Delta F_A(X) = -\rho g \Delta V(X)$ becomes

$$F = -\kappa|X|X = -\kappa X^2 \operatorname{sgn}(X), \quad (12)$$

and the acceleration, from relation (5):

$$a = -\Delta F_A(X)/\mathcal{M} = -(\kappa/\mathcal{M})|X|X, \quad (13)$$

where $\kappa = s \tan \alpha \rho g$.

A simple calculation, reported in the Appendix, proves that a quadratic restoring force produces oscillations whose period varies with amplitude as

$$T = 6.87 \sqrt{\mathcal{M}/\kappa} / \sqrt{A}. \quad (14)$$

If the triangles' vertex, in equilibrium, is placed at a distance X_0 from the water surface, the restoring force becomes asymmetric. It may be written as $\Delta F_A = \kappa[(X - X_0)|(X - X_0)| + X_0|X_0|]$, assuming $X_0 > 0$ for vertex below the free surface at equilibrium (and $X_0 < 0$ above).

Actually a real body shaped as twin triangles cannot have a zero cross section at the midpoint [$b(0) = b_0$; see Fig. 3], and therefore, even in the case of symmetric behavior ($X_0 = 0$), a linear term ($\kappa b_0 / \tan \alpha$) X in the restoring force cannot be completely avoided.

D. Oscillations of twin cones: $F = -kX^3$

If the twin triangles are replaced by twin cones (with base radius r and aperture α), the Archimedes' force has a cubic dependence on the displacement X .

With a proper choice of the counterweight, the twin cones may be set in equilibrium with their vertex at the water surface ($X_0 = 0$). In this case a simple calculation of the displaced water volume shows that the restoring force and the acceleration become, respectively,

$$F = -\xi X^3, \quad (15)$$

$$a = -(\xi/\mathcal{M})X^3, \quad (16)$$

where $\xi = \pi(\tan \alpha)^2 \rho g/3$.

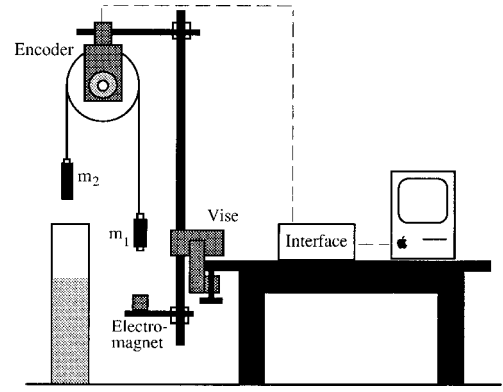


Fig. 4. Block diagram of the experimental setup.

A cubic restoring force, as shown in the Appendix, produces oscillations whose period varies with amplitude as

$$T = 7.42 \sqrt{\mathcal{M}/\xi} / A. \quad (17)$$

As for the case of real twin triangles, also for real twin cones, one has to account for the finite cross section at the joint of the cones. If r_0 is the radius at the joint, the factor X^3 in (15) and (16) becomes $[3(r_0/\tan \alpha)^2 X + 3(r_0/\tan \alpha)X^2 + X^3]$, producing an asymmetric force:

$$F = -\xi[3(r_0/\tan \alpha)^2 X + 3(r_0/\tan \alpha)X^2 + X^3], \quad (15')$$

$$a = -(\xi/\mathcal{M})[3(r_0/\tan \alpha)^2 X + 3(r_0/\tan \alpha)X^2 + X^3]. \quad (16')$$

The asymmetry, however, is small due to the fact that $r_0 \ll r$. On the contrary, when the oscillation occurs around an equilibrium position with the cone vertex *well below* the water surface (e.g., $X_0 = h/2$, where h is the cone height) the restoring force turns out to be *strongly asymmetric*. This becomes important if we use a *single cone*⁵ with amplitudes $X \leq X_0$, where the restoring force is

$$F = -\xi[(X - X_0)^3 + X_0^3] = -\xi[3X_0^2 X + 3X_0 X^2 + X^3]. \quad (18)$$

III. DATA ACQUISITION SETUP

The data acquisition system we used is based on a *Serial Interface*⁶ connecting the host computer (either a Macintosh or a PC) to a position sensor. The interface and the computer communicate by the standard serial line (RS-232). The logged data can be displayed on the computer monitor in various graphical representations using the dedicated software, which also allows one to perform numerical fits and other data handling. A real-time visualization of the kinematic variables can thus be obtained.

The position sensor is made of an optical encoder, attached to the pulley shaft⁷ that measures the pulley's rotation angle $\vartheta(t)$ from which one gets the linear displacement $X(t)$ of the hanging masses as $X = R\vartheta$ (once known as the pulley radius R).

The software calculates from the measured values of the position the corresponding values of the velocity $v(t) = dX(t)/dt$ and of the acceleration $a(t) = dv(t)/dt$.

A cheap and solid stand is provided by an aluminum tube (1 in. diam, 1.5 m long) and a vise clamped to the border of a table (Fig. 4). The tube is held vertically by screwing two metal blocks, with vertical V grooves, to the vise lips.

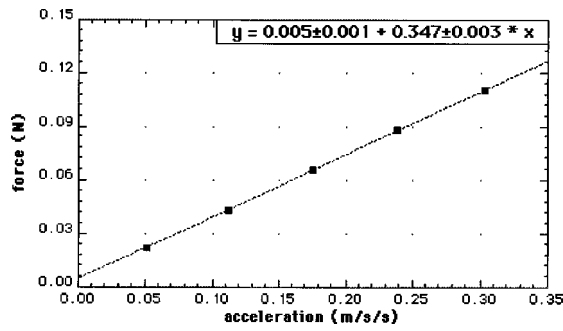


Fig. 5. Applied force F versus measured acceleration a in the classic Atwood's experiment. The best fit straight line gives both the friction force and the total inertial mass.

The pulley is a metal disk (3 mm thick, radius $R = 50$ mm) with a thin groove to keep the string (a dacron fishing wire ≈ 0.3 mm diam, $\lambda = 0.125$ g/m), and it is coaxially fixed to the rotary sensor.

The masses m_1 and m_2 are brass bodies, attached to each end of the string by means of a screw with a thin axial hole (the string can pass through the hole but a string knot is blocked). In order to avoid unwanted lateral oscillations when the motion is started, a small electromagnet can be used to block and release the counterweight m_1 (a cylinder that bears an iron screw at its bottom).

We used a perspex vessel (100 cm height and 10 cm diam) in order to make visible the whole m_2 path, but it may well be replaced by cheaper (glass or metal) vessels.

IV. SYSTEM CHARACTERIZATION (THE CLASSIC ATWOOD'S MACHINE)

Before performing the experimental study of the various type of oscillations, one needs to characterize the system by measuring the pulley's momentum of inertia I and the effective friction force F_F .

The easiest way to measure both I/R^2 and F_F is to perform a set of measurements of the acceleration where both masses move in air. In this case ($F_A = 0$) relation (6) becomes

$$\begin{aligned} a' &= (\Delta m g - F_F) / (I/R^2 + m_1 + m_2) \quad \text{or} \\ \Delta m g &= F_F + a' \mathcal{M}. \end{aligned} \quad (19)$$

That is, if the sum of the two masses ($m_1 + m_2$) is kept constant, a plot of different values of the driving force $\Delta m g = (m_2 - m_1)g$ versus the measured values of the acceleration has slope $(I/R^2 + m_1 + m_2) = \mathcal{M}$ and intercept F_F .

This experiment may be easily performed by moving a set of extra masses of known weight from one body to the other.

An example of such a plot, obtained using two equal bodies of mass 118.3 g and ten extra masses of 1.12 g each (so that $m_1 + m_2 = 247.8$ g),⁸ is shown in Fig. 5.

The experimental data show a linear behavior, thus confirming that F_F can be assumed to be constant. The best fit gives $F_F \approx (5 \pm 1) \times 10^{-3}$ N and a slope $\mathcal{M} = (0.347 \pm 0.003)$ kg. Therefore the effective inertial mass of the pulley is $I/R^2 = \mathcal{M} - (m_1 + m_2) = (0.099 \pm 0.003)$ kg.

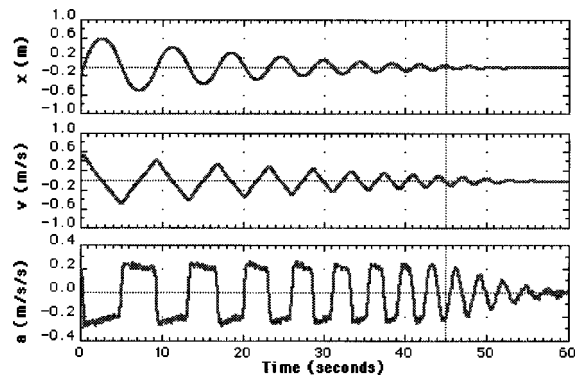


Fig. 6. Plots of position, velocity, and acceleration versus time for the cylinder oscillating inside and outside water.

V. EXPERIMENTAL INVESTIGATION OF HARMONIC AND ANHARMONIC OSCILLATIONS IN WATER

A. The case of the cylinder

Figure 6 shows the plots of position, velocity, and acceleration versus time, obtained with a brass cylinder (weight $m_2 = 143.6$ g, diameter 15 mm and height about 100 mm).⁹

The counterweight ($m_1 = 135.0$ g) was chosen so that in equilibrium the cylinder is half immersed.¹⁰ In this system the motion is expected to obey the predictions of the models described in Secs. II A (at small amplitude) and II B (at large amplitude).

After some oscillations, when the cylinder does not completely exit from water (for $t > 45$ s), the motion becomes *damped harmonic*, as clearly shown by the same plots expanded in Fig. 7.

The whole motion of the cylinder may be represented by two models: *anharmionic* oscillation prevailing in the initial phase ($t < 45$ s) and *harmonic* oscillation in the final phase ($t > 45$ s).

In plots like those shown in Figs. 6 or 7, one can use the mouse to move a vertical line (corresponding to the same value of the variable t) along all the plots, thus detecting the values of all the other variables. In this way one can easily measure the time values t_i when the acceleration changes sign ($X = 0$). The differences, $t_i - t_{i-1}$, give the values of the half-periods $T_i/2$. In the same way one can measure the values of the maximum and minimum displacements X_i , which give the amplitude A_i .

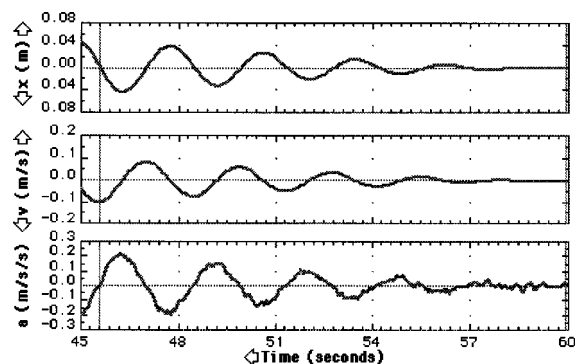


Fig. 7. An expanded plot of the data of Fig. 6 (harmonic motion).

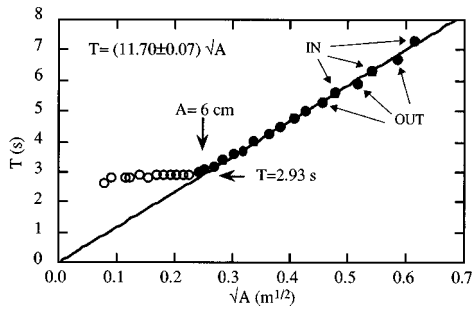


Fig. 8. Period of the cylinder oscillations as a function of the square root of amplitude. Full dots: first phase of the motion. Open dots: second phase (harmonic motion).

In Fig. 8 we report the values of the period as a function of \sqrt{A} : the full dots correspond to the first phase of the motion (the best fitting line is also drawn), while the open dots correspond to the second phase (the expected value $T = 2\pi\sqrt{\mathcal{M}/\pi\rho gr^2} = 2.93$ s of the harmonic motion is shown).

The plot shows that the period is constant for small values of the amplitude A , i.e., when the cylinder is *partially immersed* (for $A < 6$ cm), and increases linearly with \sqrt{A} at larger amplitudes. The slope predicted by relation (11): $T = 4\sqrt{2/a}\sqrt{A} = 4\sqrt{2\mathcal{M}/\Delta m g}\sqrt{A}$ is 12.0 ± 0.2 (assuming an uncertainty of 3 g on \mathcal{M} and of 0.1 g on Δm), while the value obtained by fitting the experimental data is *lower* (11.7 ± 0.1 s $m^{-1/2}$). These two values are compatible (the error bars do slightly overlap) but one may still suspect that some second-order effect was neglected.

A reduction of the measured slope with respect to the predicted one cannot be explained by considering effects such as hydrodynamic mass¹¹ (extra inertial mass due to the water displaced by the moving cylinder) because it should increase the measured slope with respect to the predicted one. The discrepancy may be explained by a small increase (say 0.2 g) of the mass difference $\Delta m = 8.6$ g. The oscillating cylinder in fact, after being dipped into the water, remains wetted by a water layer,¹² and one may even see one water drop falling just after it leaves the surface.

A direct measurement of the acceleration of the body (when it is completely inside or completely outside the wa-

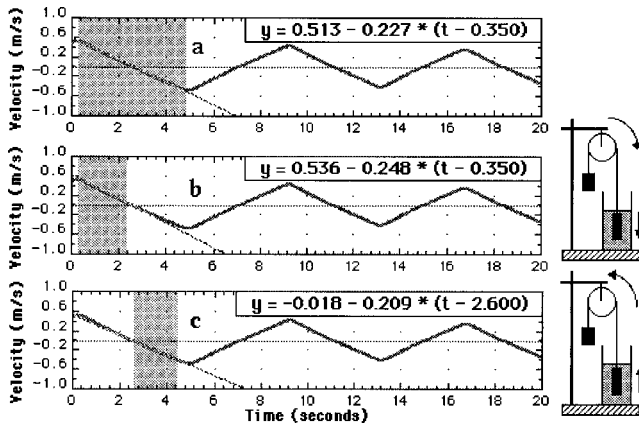


Fig. 9. Cylinder velocity plots. (a) the selected area refers to motion underwater; (b) the selected area refers to downward motion; (c) the selected area refers to upward motion.

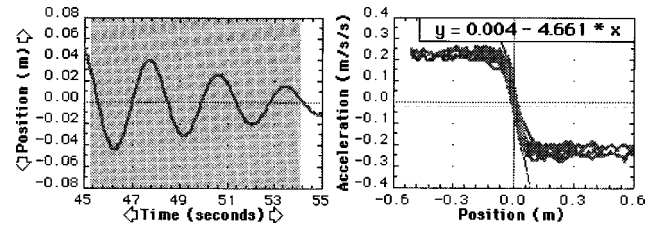


Fig. 10. Position versus time and acceleration versus position plots for the cylinder in the harmonic phase of the motion. The linear fit is made on the selected data.

ter) may be obtained as the slope of a linear fit of the velocity versus the time plot [Fig. 9(a)]. We obtain as average absolute value of the positive and of the negative slopes $a = (0.227 \pm 0.002)$ m/s^2 , to be compared with the value predicted by relation (10) $a = (0.223 \pm 0.002)$ m/s^2 . Also, here the errors bars do barely overlap, owing to the excess mass of the water film, neglected in relation (10), that is responsible for the larger observed mean acceleration.

Looking in more detail at the $v(t)$ plot, which at first sight looks like a triangular wave, we discover that the slope is slightly different in the first half and in the second half of each “quasilinear” portion of the plot. When the cylinder is inside water, the acceleration is larger when the cylinder is dipping into the water [Fig. 9(b): $a = -0.248 \pm 0.001$ m/s^2] and smaller when it is rising back toward the water surface [Fig. 9(c): $a = -0.209 \pm 0.001$ m/s^2].

The same happens when the cylinder is outside the water: here the acceleration is slightly larger when the cylinder is rising toward the top position and smaller when it is falling back toward the water surface.

The observed discontinuities Δa in the acceleration are systematic and larger than the experimental uncertainties. This feature reminds one of the behavior of a cart riding upward and downward on an incline, and it can indeed be justified by taking into account friction.

During the selected portion of motion in Fig. 9(b) the pulley rotates clockwise, while during the motion selected in Fig. 9(c) it rotates counterclockwise, and therefore the friction force has the same direction of the acceleration in the first case and the opposite one in the second case. We therefore obtain the friction force for the cylinder underwater as $F_F = \mathcal{M}(\Delta a/2) = (7 \pm 1) \times 10^{-3}$ N. When the cylinder is in air we obtain $F_F = (4 \pm 1) \times 10^{-3}$ N, in agreement with the value obtained from the plot of Fig. 5, within the experimental uncertainties.

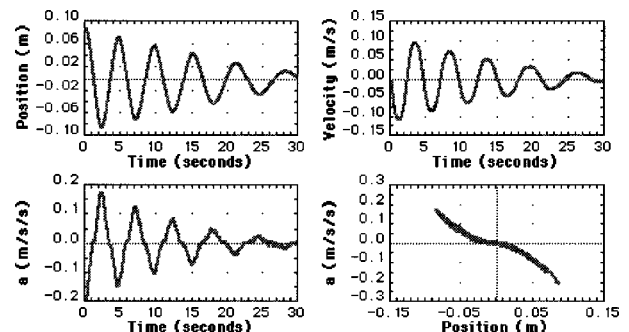


Fig. 11. Plots of position, velocity, and acceleration versus time, and acceleration versus position for the twin triangles.

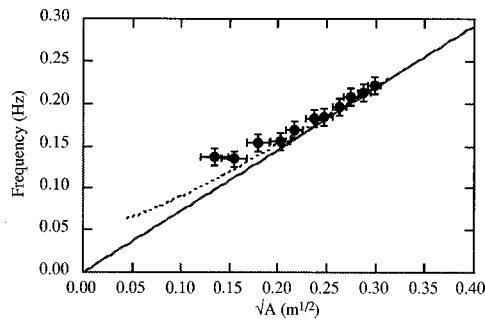


Fig. 12. Frequency of the twin triangles' oscillations as a function of the square root of amplitude. Full line: purely quadratic restoring force. Dotted line: numerical integration of the law of motion.

A larger frictional force for the cylinder underwater is consistent with the extra dissipation due to the water viscosity.

Turning to the harmonic phase of the motion, Eq. (7) gives a prediction of the slope β of the curve $a(X)$: $\beta = -k/\mathcal{M} = \pi\rho gr^2/\mathcal{M} = -4.57 \text{ s}^{-2}$. In Fig. 10 we report a fit of the central part of the plot $a(X)$ (that for $X < 6$ cm) that gives a slightly larger slope: $\beta = (-4.66 \pm 0.05) \text{ s}^{-2}$.

This discrepancy may be explained by releasing an implicit assumption that we made in our simple model. If we consider that the vessel has a relatively small inner radius ($R = 5$ cm), we may suspect that the vertical shift of the water level due to the volume of the water displaced by the cylinder immersion cannot be neglected. If we take into account this effect,¹³ by replacing the variable X with the variable $X' = X[1 + r^2/(R^2 - r^2)] = 1.023X$, the expected slope changes into $\beta = -4.67 \text{ s}^{-2}$, in excellent agreement with the measured value.

B. The case of the twin triangles

Figure 11 shows the plots of position, velocity, and acceleration versus time, and acceleration versus position obtained with brass twin triangles (with $s = 1$ cm, $h_0 = 10$ cm, $b = 4.8$ cm, $b_0 = 0.2$ cm, $m_1 = 384.8$ g, $m_2 = 408.9$ g), using a short vessel with a large inner diameter (30 cm) to make negligible the vertical shift of the water level when the body dips into the water.

Measuring the period and the amplitude, as we did for the cylinder oscillations, we obtain for the twin triangles the data shown in Fig. 12, where we plotted the frequency $f = 1/T$

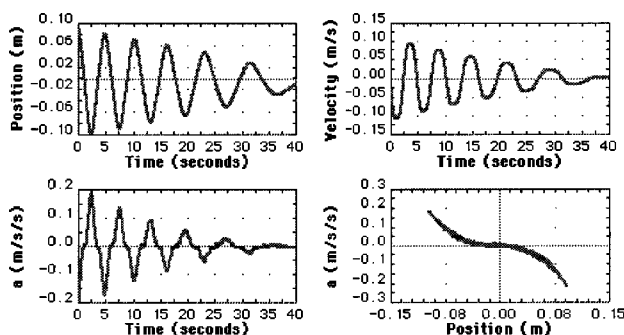


Fig. 13. Plots of position, velocity, and acceleration versus time, and acceleration versus position for the twin cones.

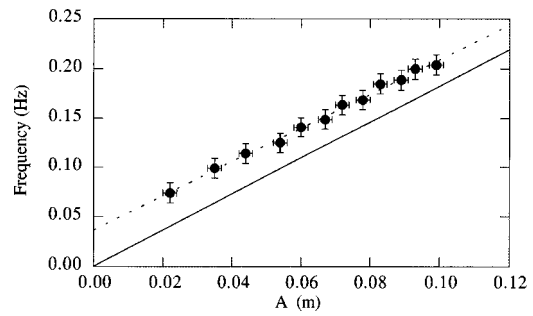


Fig. 14. Frequency of the twin cones' oscillations as a function of the amplitude. Full line: a purely cubic restoring force. Dotted line: numerical integration of the law of motion for the force $\Delta F_A(X) = \xi[X^3 + 3(r_0/\tan \alpha)X + 3(r_0/\tan \alpha)^2X^2]$.

versus the square root of the amplitude \sqrt{A} , since we expect, from Eq. (13) a linear behavior for $f(\sqrt{A})$, with a slope of $0.73 \text{ Hz}/\sqrt{\text{m}}$ (full line).

A qualitative agreement with the predicted behavior is shown indeed by the experimental results at larger amplitudes; at smaller amplitudes, however, a clear departure from the x^2 oscillator model is apparent.

A much better fit is obtained by taking into account also the linear term due to the finite thickness ($b_0 = 2$ mm) of the twin triangles at their vertex: the dotted curve in Fig. 12 represents the values of the frequency calculated, for each amplitude, by numerically integrating relation (A3), as explained in the Appendix.

C. The case of the twin cones

A record of the motion of a twin cones-shaped body (two brass cones, screwed together at their vertex, base radius $r = 1.5$ cm, height $h = 10$ cm, $m_2 = 494$ g, counterweight $m_1 = 461$ g, radius at joint $r_0 = 0.125$ cm, $\tan \alpha = 0.1375$) is shown in Fig. 13.

In the graphs we measured the values of the period and of the amplitude, and then we plotted the frequency versus the amplitude, as we expect the behavior predicted by Eq. (16):

$$f = 0.135 \sqrt{\xi/\mathcal{M}A} = 0.135 \sqrt{\pi(\tan \alpha)^2 \rho g / (3\mathcal{M})A}. \quad (20)$$

In Fig. 14 we have drawn the straight line representing the expected behavior for a purely cubic restoring force (a full line with slope $1.83A$ Hz/m). The dotted curve represents the numerical integration of the law of motion (see the Appendix) that assumes a restoring force which includes also the linear and the quadratic term predicted by Eq. (15'): $F(X) = -\xi[X^3 + 3(r_0/\tan \alpha)X + 3(r_0/\tan \alpha)^2X^2]$, where r_0 is the radius of the cross section of the twin cones vertex.

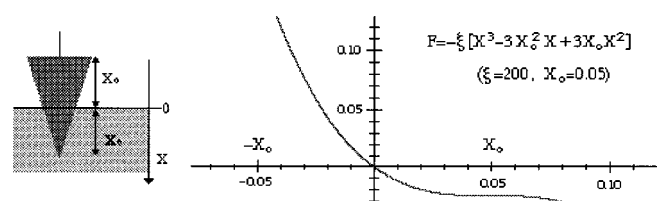


Fig. 15. Behavior of the expected restoring force for a single cone.

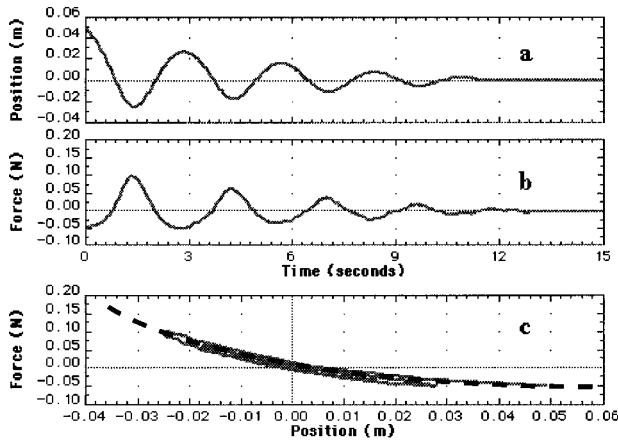


Fig. 16. Plot of position (a) and restoring force (b) vs time for the single cone. Plot of force versus position (c): the dotted line represents the fitting function $F = -\xi[(X - X_0)^3 + X_0^3]$.

D. The case of a single cone: a macroscopic model of the atomic vibration in solids

The analysis made in Sec. II D shows that for a single cone of height h , in equilibrium at half height ($X_0 \approx h/2$), the restoring force becomes $-\Delta F_A = -\xi[(X - X_0)^3 + X_0^3]$, with $-X_0 < X < X_0$, and $\xi = \pi(\tan \alpha)^2 \rho g/3$. The geometry of this system, with the expected shape of the restoring force is shown in Fig. 15.

Comparing this system to the well-known mass-spring system, we note here that the *spring stiffness* is no longer constant: it increases for $X > 0$ and decreases for $X < 0$. In the real world these kinds of forces are much more common than one might suppose at first sight. The cohesive force in solids is the simplest example. Short-range repulsion (the “hard sphere interaction” due to the Pauli exclusion principle) varies with displacement (with respect to the equilibrium position of the atoms) much faster than long range attraction (the van der Waals interaction due to polarization). Therefore the atoms’ vibration in a crystal lattice is more closely approximated by the motion of a cone-shaped body floating in a liquid bath than by the usual mass-spring system. In fact, only the *asymmetry* of the restoring force (and of the related potential curve) may explain the positive thermal expansion coefficient:¹⁴ a symmetric restoring force would give instead *zero* thermal expansion coefficient.

If we unscrew the twin cones and change the counterweight in order to keep in equilibrium (half immersed) one single cone, the recorded oscillation is indeed asymmetric [Fig. 16(a)]. The restoring force may be calculated from the measured acceleration as $F(t) = \mathcal{M}a(t)$, knowing that the inertial mass is now 0.544 kg. The calculated values [Fig. 16(b)] of the variable $F(t)$ may be plotted versus the corresponding values of the variable $X(t)$ [Fig. 16(c)]. In this plot, the slope corresponds to the elastic constant in the mass-spring system, and it is here larger for $X < 0$ than for $X > 0$. In the same plot the dashed line represents the values of the function $F = -\xi[(X - X_0)^3 + X_0^3]$, calculated with the nominal values $\xi = 200 \text{ N/m}^3$ and $X_0 = 0.05 \text{ m}$.

VI. CONCLUSIONS

The experimental results reported in this paper show that a MBL version of the Atwood’s machine is a simple and powerful device for investigating various kind of motions.

In particular, it can be used to introduce the students to the study of harmonic and anharmonic oscillations, the required physics background being restricted to elementary mechanics.

At the introductory level, the study of nonlinear oscillators appears to be important in order to provide the students with examples of asymmetric restoring forces that are necessary to model the real behavior of solids, e.g., the nonzero thermal expansion coefficient.

The apparatus described here combines efficiently the advantages of the Atwood’s machine and those of the MBL acquisition system. The Atwood’s machine is suitable for introductory level investigations because the basic features of the system influencing the motion of the bodies can be easily identified (and modified) by the students themselves. The data acquisition system can be a powerful cognitive tool by allowing a real time visualization of the relevant variables selected by the students according to any particular model they wish to test, and by encouraging the students to play the game of gradually refining the schematization in order to reach a satisfactory agreement with experimental data. The data accuracy that can be achieved with MBL is such to make the refinements possible and testable, as shown in the present paper.

APPENDIX: THE CALCULATED DEPENDENCE OF PERIOD FROM AMPLITUDE

A simple dimensional argument that yields the correct dependence of the period T from the amplitude A in a generic oscillation driven by a restoring force of the type $F = -kx^n$ is the following. The period may depend only on the quantities

$$m \text{ (kg)}, \quad k \text{ [N/m}^{-n} = \text{kg m}^{1-n} \text{ s}^{-2}], \quad A \text{ (m)}.$$

The only combinations of these quantities with the dimensions of time, for different values of n , are $\sqrt{m/k}$ for $n=1$, $\sqrt{m/kA}$ for $n=2$ and $\sqrt{m/kA^2}$ for $n=3$. Therefore the period must be *proportional to* $\sqrt{m/k}$, $\sqrt{m/k}/\sqrt{A}$, and $\sqrt{m/k}/A$, respectively.

The proportionality constant must obviously be derived by a different method.¹⁵

The change in kinetic energy ΔE [between $v=0$ for $x=x_0$, and the generic $v(x)$ for $x \leq A$] equals the work done by the restoring force, and therefore we may write

$$\frac{1}{2} m v^2(x) = \int_{x_0}^x F(x) dx. \quad (\text{A1})$$

By solving this equation with respect to the velocity, we get

$$v(x) = \pm \sqrt{2 \int_{x_0}^x \frac{F(x)}{m} dx} = \frac{dx}{dt} \quad \text{or} \quad (\text{A2})$$

$$dt = \frac{dx}{\pm \sqrt{\frac{2}{m} \int_{x_0}^x F(x) dx}}.$$

The integral in the last equation from the time of maximum displacement ($x_0 = A$) to the time when the system is in equilibrium ($x = 0$) gives the value $T/4$, and therefore the period T is

$$T = 4 \int_A^0 \frac{dx}{-\sqrt{\frac{2}{m} \int_A^x F(x) dx}} \quad (\text{A3})$$

(the minus sign in the last equation is due to the fact that when the body approaches equilibrium its velocity is negative). We may use this equation to calculate the period of an oscillation due to a restoring force of the kind: $F = -kx^n$,

$$\begin{aligned} T &= 4 \int_A^0 \frac{dx}{-\sqrt{\frac{2}{m} \int_A^x (-kx^n) dx}} \\ &= 2 \sqrt{\frac{m}{k}} \int_A^0 \frac{dx}{\sqrt{\int_A^x x^n dx}}. \end{aligned} \quad (\text{A4})$$

The case of SHM ($n=1$) may be integrated analytically, leading to the known result $T = 2\pi\sqrt{m/k}$, and for the restoring force $F = -k \operatorname{sgn} X$ we find $T = 4\sqrt{2m/k}\sqrt{A}$.

In the case of the twin triangles ($n=2$) and twin cones ($n=3$) we may use instead numerical integration, obtaining $T = 6.87\sqrt{m/k}/\sqrt{A}$, and $T = 7.42\sqrt{m/k}/A$, respectively. We used the function "Nintegrate" within the standard "MATHEMATICA" software package.¹⁶

Numerical integration may be easily performed also when the restoring force has a polynomial form as for real twin triangles and twin cones, which cannot have a zero cross section at the vertex.

³Also at Istituto di Chimica e Tecnologie Inorganiche e Materiali Avanzati (ICTIMA—Consiglio Nazionale delle Ricerche), Padova, Italy.

¹From now on, the constants $k, k', k'', \kappa, \kappa'$... will be assumed to be positive.

²Several experimental setups have been proposed to investigate the " x^3 " oscillator with a mass-spring system: e.g., J. Thomchick and J. P. McKelvey, "Anharmonic vibrations of an ideal Hooke's law oscillator," *Am. J. Phys.* **46**, 40–45 (1978); S. Whineray, "A cube-law air track oscillator," *Eur. J. Phys.* **12**, 90–95 (1991); A. Cromer, "The x^3 oscillator," *Phys. Teach.* **30**, 249–250 (1992); N. C. Bobillo-Ares and J. Fernandez-Nunez, "Two-dimensional harmonic oscillator on air table," *Eur. J. Phys.* **16**, 223–227 (1995).

³When also the string's mass cannot be neglected, the maximum relative correction to the acceleration value (4) is $2\lambda y/\Delta m$, where λ is the linear density of the wire and y is the distance of each mass from the equilibrium position the acceleration being $a = [(\Delta m + 2\lambda y)g - F_A]/[(2L + \pi R)\lambda + \mathcal{M}]$, where L is the string length [C. T. P. Wang, "The improved determination of acceleration in the Atwood machine," *Am. J. Phys.* **41**, 917–919 (1973)]. For large cross-section dipped bodies also the hydrodynamic mass $m_h = km_2$ should be taken into account: this, however, requires the calculation of the geometrical factor k that depends on the body shape.

⁴A detailed analysis of this kind of motion was made by I. R. Gatland, "Theory of a nonharmonic oscillator," *Am. J. Phys.* **59**, 155–158 (1991).

⁵We therefore disagree with the analysis reported by A. Jafari ["Experimental test of $F = -kx^n$," *Phys. Teach.* **34**, 196 (1996)], where he claims that a single cone would produce a purely cubic restoring force.

⁶The data and graphics reported in this paper were taken with an interface (model ULI-II) produced by Vernier Software (Portland, OR), but similar performances were obtained using an equivalent interface (model 500) produced by PASCO (Roseville, CA).

⁷The "Rotary motion sensor" is available both from Vernier Software and PASCO. A similar device can be home built using one of the encoders contained in the "mouse" that comes with any PC, as explained by O. Ocho and N. F. Kolp, "The computer mouse as data acquisition interface," *Am. J. Phys.* **65**, 1115–1118 (1997).

⁸We used an electronic balance with an accuracy of 0.1 g to measure the weight of ten equal metal washers for a total of 11.2 g. Each time one extra mass m is displaced from one body to the other, the force changes by the quantity $F = 2mg = 0.0224$ N.

⁹The cylinder top and bottom have spherical shape in order to reduce the oscillation damping.

¹⁰This "mass trimming" is obtained by using small lead spheres (those normally used to load fishing wires) that were clamped to the wire above the counterweight.

¹¹An order of magnitude of the hydrodynamic mass m_h may be calculated, following K. Thompson ["Hydrodynamic mass," *Am. J. Phys.* **56**, 1043 (1988)], with the simplified assumption of a long cylinder moving end on: $m_h = (\rho_w/\rho_b)(2r/L)[\ln(L/r) - 1]m_2$, where ρ_w and ρ_b are the densities of water and brass, respectively. In our case we get a mass correction (m_h/\mathcal{M}) of about 2%.

¹²This effect can also be detected by a careful inspection of the plot of Fig. 8. The full circles belong alternately to straight lines with different slopes: those marked "OUT" are the period values calculated from half-periods spent "out of water" (an expected smaller slope) while those marked "IN" are calculated from half-periods "inside water" (an expected larger slope).

¹³This can also be detected by a careful eye inspection because the free water surface moves up and down by about 1.3 mm.

¹⁴V. F. Weisskopf and H. Bernstein, "Search for simplicity: Thermal expansion," *Am. J. Phys.* **53**, 1140–1141 (1985).

¹⁵See, for example, C. Hirata and D. Thiessen, "The period of $F = -kx^n$ harmonic motion," *Phys. Teach.* **33**, 562–564 (1995).

¹⁶Available for Macintosh and PC-IBM from Wolfram Research (at low cost in the Education version for teachers and students).

MEMORY LOSS

Physics is largely an attitude of mind and I like to think that if I should go to bed tonight and wake up in the morning to find that I had forgotten everything that I had ever learned, but had succeeded in retaining such experience as I have in thinking, I should not have suffered very much by the loss. It would, of course, be a little inconvenient to fail to have ready at hand some of the formulas and methods which are so familiar to us, but this loss could soon be repaired.

W. F. G. Swann, "The Teaching of Physics," *Am. J. Phys.* **19**(3), 182–187 (1951).